Research, Univ. of Texas, Austin, CFHR Res. Rept. 98-1, Jan. 1968.
18. J.F. Shook and B.F. Kallas. Factors Influencing Dynamic Modulus of Asphalt Concrete. Proc., AAPT, Vol. 38, 1969.
19. W.H. Gotolski, S.K. Ciesielski, and L.N. Heagy. Progress Report on Changing Asphalt Properties of In-Service Pavements in Pennsylvania. Proc., AAPT, Vol. 33, Feb. 1964, pp. 285-319.
20. W.J. Kenis. Progress Report on Changes in Asphaltic Concrete in Service. HRB, Bull. 333, 1962, pp. 39-65.
21. W.J. Liddle, G.M. Jones, and D.E. Peterson. Use of Synthetic Rubber-in-Asphalt Pavement to Determine Mixture Behavior and Pavement Performance. Materials and Tests Division, Utah State Highway Department, Interim Rept. Utah Project HPR 1 (8), BPR Studies 10 and 14; State Studies 903 and 910, Dec. 1979.
22. W.E. Simpson, R.L. Griffin, and T.K. Miles. Correlation of the Microfilm Durability Test with Field Hardening Observed in the Zaca-Wigmore Experiment Project. Symposium on Paving Materials, ASTM Special Tech. Publ. 277, 1959, pp. 52-63.
23. J. Skog. Results of Cooperative Test Series on Asphalts from the Zaca-Wigmore Experimental Project. Symposium on Paving Materials, ASTM Special Tech. Publ. 277, 1959, pp. 46-51.
24. E. Zube and J. Skog. Final Report on the Zaca-Wigmore Asphalt Test Road. Materials and Research Department, Division of Highways, California Department of Transportation, Sacramento, 1959.
25. L.W. Corbett and R.E. Merz. Asphalt Binder Hardening in the Michigan Test Road After 18 Years of Service. TRB, Transportation Research Record 544, 1975, pp. 27-34.
26. R.J. Schmidt. Use of ASTM Tests to Predict Low-Temperature Stiffness of Asphalt Mixes. TRB, Transportation Research Record 544, 1975, pp. 46-55.
27. Local Climatological Data: Annual Summaries for 1977. National Oceanic and Atmospheric Administration, Rockville, MD, 1978.
28. F.L. Roberts, T.W. Kennedy, and G.E. Elkins. Material Properties to Minimize Distress in Zero-Maintenance Pavements. Federal Highway Administration, U.S. Department of Transportation, Draft Final Rept., Aug. 1979.
29. R.C.G. Haas. A Method for Designing Asphalt Pavements to Minimize Low-Temperature Shrinkage Cracking. Asphalt Institute, College Park, MD, Res. Rept. 73-1, Jan. 1973.
30. N.W. McLeod. Prepared Discussion on Ste. Anne Test Road. Proc., Canadian Technical Asphalt Association, 1969.

Publication of this paper sponsored by Committee on Flexible Pavement Design.

Distress Behavior of Flexible Pavements That Contain Stabilized Base Courses

M. C. WANG AND W. L. GRAMLING

The distress behavior of full-scale experimental pavements is analyzed and discussed. The pavements contained five different base-course materials, namely, bituminous concrete, aggregate cement, aggregate-lime-pozzolan, aggregate bituminous, and crushed stone. Three types of aggregate—limestone, slag, and gravel—were used in the aggregate-cement base. Distress behavior discussed includes rutting, surface roughness, and cracking. Distress behavior observed is related to the pavement response, which was analyzed by using the BISAR computer program. The critical responses analyzed are maximum tensile strain at the bottom of the base course and maximum compressive strain at the top of the subgrade. Various equations relating distress and response are established that permit prediction of the amount of rutting, roughness, and cracking, and allowable subgrade compressive strains to limit different distress modes within specified levels are also established. Field distress data are also related to the present-serviceability-index (PSI) values of each test pavement. From these relationships, various levels of each mode of distress manifestation are established for each level of PSI drop. Results obtained from this study may be useful in selecting allowable distress levels and allowable subgrade compressive strain for pavement design and can also be helpful in developing the relationship between distress and performance.

Distress is related to structural defects that result from a variety of traffic- and environment-related causes; it may affect pavement performance directly or indirectly. In general, distress takes one of three forms—fracture, distortion, or disintegration. The distress mechanisms that contribute most significantly to a reduction in pavement serviceability, according to Finn (1), are fatigue cracking, rutting and slope variance, and cracking caused by shrinkage or by changes in temperature and subgrade moisture.

To design a pavement structure that will be maintenance-free within a design period of normally 20 years requires a thorough understanding of distress behavior and an ability to predict the degree of various distress manifestations. To date, a number of mathematical distress models have been developed for flexible pavements. An extensive list of these models is given by Rauhut, Roberts, and Kennedy (2). Some models capable of predicting rutting, fatigue cracking, and low-temperature cracking are VESYS A (3), PDMAP (4), the Shell method (5), and WATMODE (6). Some of these models were developed from statistical analysis of field data and thus require modification for use under other loading, environmental, and material conditions. Others were developed with assumptions to simplify loading and structure conditions and require field data for calibration and validation.

This paper discusses the distress behavior of several types of pavements studied at the Pennsylvania Transportation Research Facility, and various equations that relate distress and response variables are developed. These equations permit prediction of the degree of different distress manifestations and also provide data useful for relating distress and performance.

EXPERIMENTAL PAVEMENTS

The Pennsylvania Transportation Research Facility is a 1.6-km (1-mile), one-lane, 3.7-m (12-ft) wide test road that was constructed in the summer of 1972. The original facility consisted of 17 sections; each section contained either different base-course materials with the same layer thicknesses or one type of base-course material with

different layer thicknesses. In the fall of 1975, one section (section 8) was overlaid, and four sections (sections 10-13) were replaced by eight shorter sections, as shown in Figure 1.

The wearing surface was an ID-2A bituminous concrete. The subbase material was a crushed limestone. The subgrade soil was a silty clay that had classifications from A-4 to A-7. The base-course materials were bituminous concrete, aggregate cement, aggregate-lime-pozzolan, aggregate bituminous, and crushed stone. Three types of aggregate were used in the aggregate-cement base--limestone, slag, and gravel. Although three different base thicknesses were available for the aggregate-lime-pozzolan base, the pavements with bases that were 10.1 cm (4 in) and 15.2 cm (6 in) thick, i.e., sections F and G, were unable to cure properly due to cold weather during construction. Thus, these two sections were excluded from this analysis.

The traffic on the facility was provided by a conventional truck tractor pulling a semitrailer and one or two full trailers. The pavements constructed in 1972 had been subjected to about 2.4 million applications of 80-kN (18-kip) equivalent single-axle loads (EALs), whereas the pavements constructed in 1975 had received about 1.3 million EALs by the end of May 1978. Complete information on design, construction, and traffic operation is documented elsewhere (7,8).

FIELD TESTING

Rut depth was measured biweekly every 12.2 m (40 ft) in both wheel paths by using an A-frame that was attached to a base channel 2.1 m (7 ft) long. Surface cracking was surveyed and mapped biweekly. Surface roughness was measured in both wheel paths by using a MacBeth profilograph. The roughness factors obtained from the profilograph data were converted into the present serviceability index (PSI) of the pavement by using the following equations:

$$PSI = 11.33 - 4.06(\log RF) - 0.01\sqrt{C + P} - 0.21\overline{RD}^2 \quad (1)$$

$$RF = 63.267 + 0.686R \quad (2)$$

where

RF = Mays road-meter roughness factor,
C = area of cracking (m^2/1000 m^2),
P = area of patching (m^2/1000 m^2),
$\overline{RD}$ = average rut depth (cm), and
R = profilograph readings (cm/km).

Figure 1. Plan view and longitudinal profile of test track.

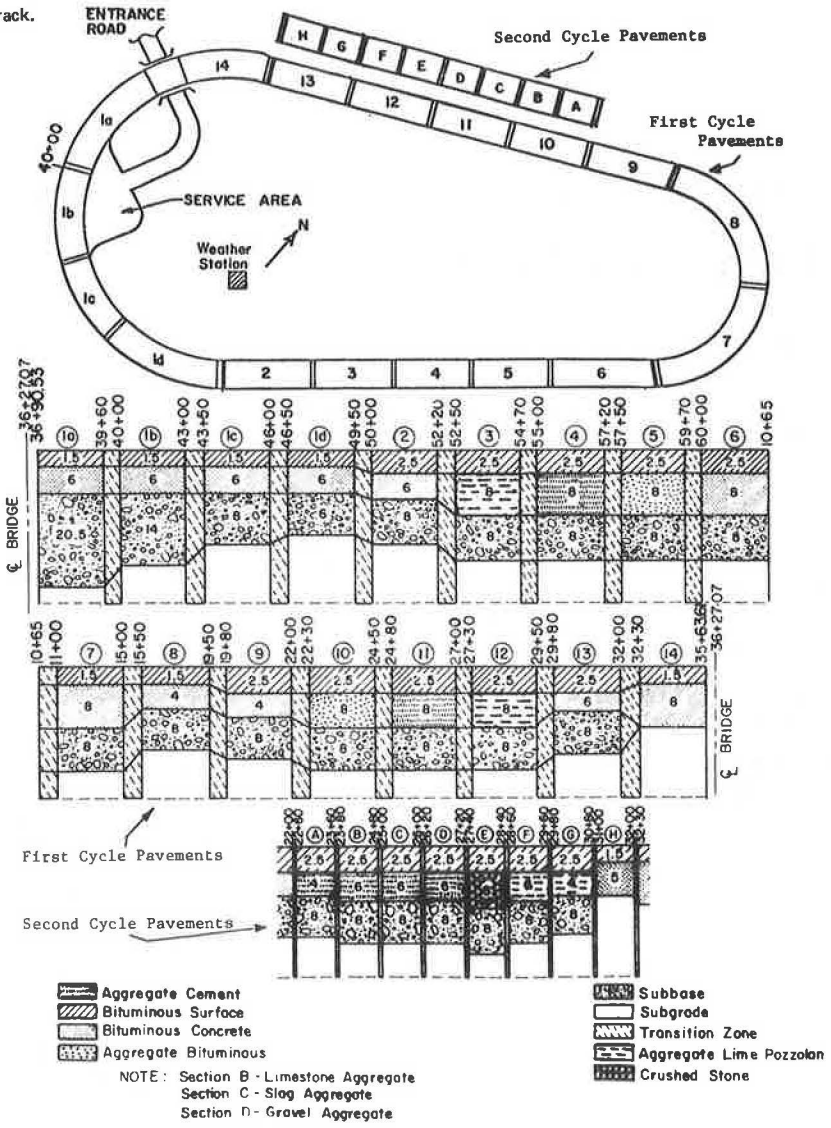

Table 1. Elastic constants and fatigue properties of pavement materials for spring weather conditions.

Layer	Material	Elastic Modulus (MPa)	Poisson's Ratio	Fatigue Constants K_1	Fatigue Constants K_2
Surface	Bituminous concrete	966	0.40	4.66×10^{-7}	3.61
Base	Bituminous concrete	2 207	0.35	1.06×10^{-6}	3.14
	Limestone aggregate cement	24 828	0.20	6.56×10^{-21}	6.05
	Slag aggregate cement	22 069	0.20	4.48×10^{-9}	3.08
	Gravel aggregate cement	17 241	0.20	1.83×10^{-8}	2.93
	Aggregate-lime-pozzolan	16 552	0.15	2.80×10^{-4}	2.17
	Aggregate bituminous	690	0.35	–	–
Subbase	Crushed limestone	331	0.40	–	–
Subgrade	Silty clay	55	0.45	–	–

Notes: 1 MPa = 145 lbf/in^2. Fatigue equation: $N_i = K_1(1/\epsilon)^{K_2}$.

These two equations were developed by Hopkins (9) of the Pennsylvania Department of Transportation.

In addition, surface deflections were measured in the wheel paths by using the Benkelman beam and the road rater. Pavement temperature profile and subgrade moisture distribution were measured by using thermocouples and moisture cells. Also, two frost-depth indicators were installed at the research facility to measure the depth of frost penetration. Weather data such as wind velocity, precipitation, and temperature were collected by using various meteorological gages.

MATERIAL PROPERTIES

The composition, gradation, and index properties of the constituent material of each pavement are documented in a research report (7). The modulus of elasticity of each layer was determined by using laboratory repeated-load tests on laboratory-compacted test specimens. The specimens had a diameter of 15.2 cm (6 in) and a height of 25.4 cm (10 in). The repeated load had a frequency of 20 cycles/min and a duration of 0.1 s. The modulus values obtained for the spring weather conditions are summarized in Table 1. In the spring season, the average pavement temperature was approximately 15.6°C (60°F), and the average subgrade moisture content was about 23 percent.

Data on the change of modulus values with the number of axle-load applications are required for determination of the variation in pavement response during the pavement's service life. For this purpose, regression analyses were performed for the Benkelman-beam deflection data. Results of the analyses were equations that related deflection with influential factors such as the number of EALs, pavement temperature, and subgrade moisture. The complete deflection equations can be found elsewhere (10). These deflection equations permit calculation of spring season deflections at any time for all experimental pavements except sections 1a, F, and G. On the basis of the computed spring season deflections, the modulus of elasticity of the combined surface and base layer at any number of axle-load applications was determined by using the bitumen-structures-analysis-in-roads (BISAR) computer program. In the determination, an assumption was made that the subgrade and subbase moduli remained constant through the entire service life of the experimental pavements. This assumption was also adopted in a previous study (11).

Fatigue properties of the surface and base-course materials were determined by conducting fatigue tests on laboratory-compacted beam specimens. The repeated loading had the same frequency and duration as that used in the testing of the resilient modulus. The test results are included in Table 1. Note that, because of the difficulty in preparing aggregate-bituminous test specimens, no fatigue data for this base-course material are given. Also contained in Table 1 is Poisson's ratio for each pavement constituent material. These ratios were obtained from other studies (12-14).

PAVEMENT RESPONSE

The response of the test pavements to traffic loading was analyzed by using the BISAR computer program and the material properties described previously. The traffic loading used had an 80-kN dual-wheel single-axle load and a 55-kPa (80-lbf/in^2) tire pressure. The analysis was made for spring weather conditions only. In the analysis for tensile strain variation with EAL, the surface and base courses were combined into one layer. For the analysis of initial pavement conditions, the surface and base layers were treated individually.

The critical responses analyzed were maximum tensile strain at the bottom of the base layer and maximum vertical compressive strain in the subgrade. The critical responses analyzed for initial pavement conditions were later related to the distress and performance data collected from the research facility.

RUTTING BEHAVIOR

As expected, rut depth increased with increasing number of 80-kN EAL applications. The rate of increase varies with many factors, such as base-course material, layer thickness, and axle-load applications. For the same base-course material, the pavement with a thick base course displays less rutting, as would be expected. Figure 2 shows the rut data for different base-course materials with the same 15.2-cm thickness. It can be seen that in the early stage the amount of rutting increases with the type of base-course material in the following order: aggregate cement, aggregate-lime-pozzolan, bituminous concrete, aggregate bituminous, and crushed stone. After about 1.2 million EALs, however, rutting in the aggregate-lime-pozzolan pavement surpasses that in other stabilized base pavements. A possible reason for this observation will be discussed.

Rutting is primarily a result of permanent deformation of each pavement constituent layer and the subgrade soil. Among the four stabilized base-course materials studied, aggregate cement and aggregate-lime-pozzolan are more rigid and brittle than bituminous-concrete and aggregate-bituminous base courses. The brittle nature gives smaller permanent deformations in the aggregate cement and aggregate-lime-pozzolan base courses, and the greater rigidity results in a smaller compressive stress at the top of the subgrade. The lower compressive stress on the top of the subgrade induces a smaller permanent deformation in the subgrade. As a consequence, both aggregate-cement and aggregate-lime-pozzolan pavements undergo less rutting than bituminous-concrete and aggregate-bituminous pavements while the pavements are in a structurally sound condition. The cracking data presented later indicate that, after about 2.4 million EALs, (a) surface cracking developed in both wheel paths throughout the entire aggregate-lime-pozzolan pavements, (b) the intensity of surface cracking in the aggregate bituminous pavement was much less, (c) only slight class 1 cracking developed in the aggregate-cement pavement, and (d) no apparent surface cracking was observed in the bituminous-concrete pavement. Because of the intensive cracking in the aggregate-lime-pozzolan

pavements, the stiffness of the surface and base layers decreased and the compressive stress in the subgrade increased. Consequently, rutting in the aggregate-lime-pozzolan pavement increased fastest among the four stabilized base pavements during the later stage of their service life.

Also shown in Figure 2 are seasons within which the rut-depth data were taken. No clear indication is seen that rutting varied significantly with season, as reported by Saraf, Smith, and Finn (15).

The rut-depth data for the three pavements that contained a 15.2-cm aggregate-cement base indicate that, among the three types of aggregate studied, limestone has the greatest resistance to rutting, slag has an intermediate level, and gravel has the least. This is probably due to the difference in the resilient modulus, which is greatest for limestone, intermediate for slag, and least for gravel, as shown in Table 1. A detailed discussion of the rutting behavior of the three types of aggregate can be found elsewhere (16).

The relationship between rut depth and the number of EALs was formulated by using the curve-fitting process. Results of the analysis give the following equation:

$$\overline{RD} = 2.54c_1(N)^{c_2} \quad (3)$$

where N = the number of 80-kN EALs (000 000s) and c_1, c_2 = coefficients. Coefficients c_1 and c_2 are given in Table 2 for all test pavements except section 1a. This section is not included because it was disturbed by the construction of the bridge and was overloaded by the equipment used for the bridge testing. Both c_1 and c_2 can be expressed in terms of the maximum compressive strain on the top of the subgrade (ε_V) as follows.

For bituminous-concrete and aggregate-bituminous pavements: $\log c_1 = 260\,\varepsilon_V^2 - 1.137$, $\log c_2 = 0.028\sqrt{\varepsilon_V} - 0.474$.
For limestone-aggregate cement and aggregate-lime-pozzolan pavements: $\log c_1 = 1020\,\varepsilon_V^2 - 1.076$, $\log c_2 = 0.028\sqrt{\varepsilon_V} - 0.274$.
For gravel and slag aggregate-cement pavements: $\log c_1 = 1080\,\varepsilon_V^2 - 0.754$, $\log c_2 = 0.028\sqrt{\varepsilon_V} - 0.274$.

Because more data points for pavements that contain bituminous-concrete base-course material are available for the development of the preceding equations, the first two calculations may provide better relations than others. A fairly good agreement between the calculations and the field data is shown in Figure 2.

The number of 80-kN EALs required to produce a rut depth is related to the initial maximum compressive strain on the top of the subgrade in Figure 3. It is interesting to note that the data points for the aggregate-bituminous pavement fall within the group of data points for the bituminous-concrete pavements, while those of the aggregate-lime-pozzolan pavements are located inside the group of the aggregate-cement pavements. The figure indicates the values of allowable maximum compressive strain so that rutting will not exceed any specified limit. For example, to limit rutting within 6.4 mm (0.25 in) after 1 million EALs, the allowable maximum compressive strain equals about 180 μm/m for the gravel-aggregate cement, slag-aggregate cement, and aggregate-lime-pozzolan pavements and approximately 230 μm/m for the limestone-aggregate cement pavements. For the bituminous-concrete and aggregate-bituminous pavements, the maximum compressive strain required to limit rutting within 6.4, 12.8, and 17.2 mm (0.25, 0.50, and 0.75 in) with 1 million EALs is 450, 550, and 600 μm/m, respectively. These allowable maximum compressive strains constitute a strain criterion for preventing excessive rutting in a newly designed pavement.

Figure 2. Rut depth versus EAL for different base-course materials.

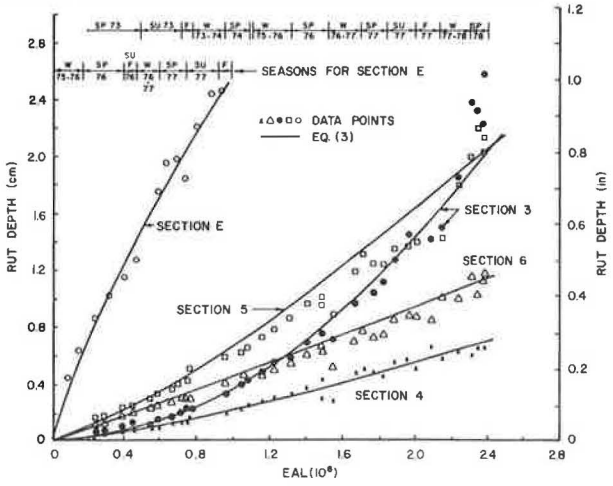

ROUGHNESS BEHAVIOR

Surface roughness, which is measured in terms of profilograph readings, increases with increasing number of EALs, as would be expected. Figure 4 compares the change of roughness with EALs for the different base-course

Table 2. Coefficients of rut depth and roughness equations.

Base	Section	Maximum Compressive Strain (μm/m)	Coefficients			
			c_1	c_2	m_1	m_2
Bituminous concrete	1b	294.2	0.12	1.41	78.97	0.23
	1c	426.6	0.16	1.41	64.96	0.23
	1d	483.0	0.22	1.41	74.48	0.31
	2	383.6	0.14	1.25	46.28	0.22
	6	291.6	0.18	1.05	69.43	0.22
	7	322.4	0.18	1.05	75.31	0.38
	8	594.0	0.57	1.62	103.88	0.47
	9	525.8	0.50	1.25	46.53	0.78
	H	884.8	8.10	2.50	107.77	0.42
	14	390.9	0.17	2.32	132.42	0.22
Aggregate cement	4	107.5	0.09	1.30	30.98	0.68
	A	288.0	0.50	1.37	62.26	1.04
	B	171.5	0.19	0.95	207.43	1.51
	C	185.5	0.43	1.35	50.65	1.23
	D	216.0	0.55	1.70	100.29	1.23
Aggregate-lime-pozzolan	3	142.8	0.18	1.77	56.12	1.12
Aggregate bituminous	5	403.0	0.27	1.26	44.20	0.46
Crushed stone	E	575.4	1.00	0.80	43.29	1.05

Note: 1 μm/m = 1 × 10^{-6} in/in.

materials studied. In general, the difference in roughness behavior among the various base-course materials and aggregate types studied is similar to that of rutting behavior. Meanwhile, no significant variation in surface roughness between seasons has been observed for the pavements under investigation.

Figure 5 shows the relation between the maximum compressive strain on the top of the subgrade and the number of EALs required to produce a certain level of surface roughness. According to this figure, the maximum allowable compressive strains to limit surface roughness at 1 million EALs within 15.8, 31.6, and 57.3 cm/km (10, 20, and 30 in/mile) are roughly 140, 170, and 190 μm/m, respectively, for the aggregate-cement and aggregate-lime-pozzolan pavements. For the bituminous-concrete and aggregate-bituminous pavements, the allowable maximum compressive strains are approximately 330, 400, and 460 μm/m, respectively, for 15.8, 31.6, and 57.3 cm/km with 1 million EALs.

Typical relationships between surface roughness and rutting are shown in Figure 6. The well-defined linear relation in the logarithmic scale suggests the following equation:

$$R = m_1(\overline{RD})^{m_2} \quad (4)$$

where R = surface roughness (cm/km) and m_1, m_2 = coefficients. The values of coefficients m_1 and m_2 are tabulated with the coefficients of Equation 3 in Table 2. The table reveals that both m_1 and m_2 increase with an increase in the compressive strain.

CRACKING BEHAVIOR

Transverse shrinkage cracking developed across the entire width in all aggregate-cement pavements except section 11, which contained a 20.3-cm (8-in) limestone-aggregate cement base course and was removed after about 1.1 million EALs. This shrinkage cracking was observed earlier than load-associated cracking. In most cases, the presence of shrinkage cracking aided, in varying degrees, the growth of load-associated cracking. More detailed information on cracking in the aggregate-cement pavements is available elsewhere (16). Transverse temperature cracking appeared

Figure 3. Initial maximum compressive strain versus EAL at different rut depths.

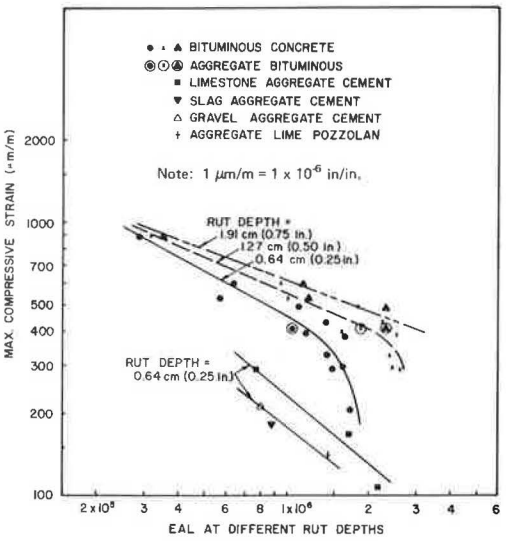

Figure 4. Roughness versus EALs for different base-course materials.

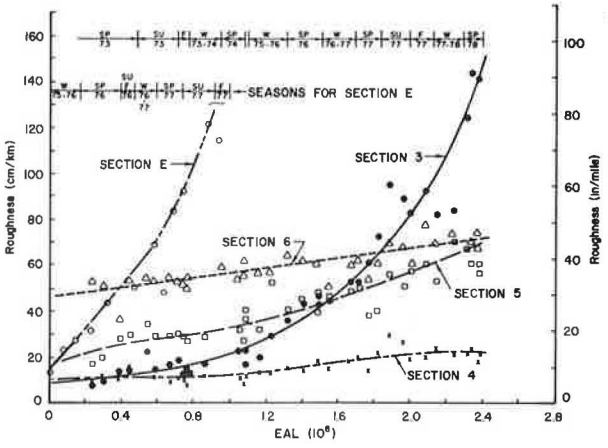

Figure 5. Initial maximum compressive strain versus EALs for various levels of roughness.

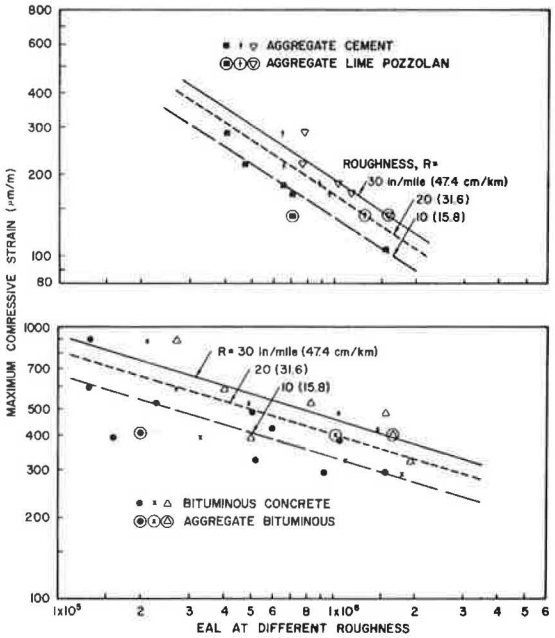

Figure 6. Relationship between rut depth and roughness.

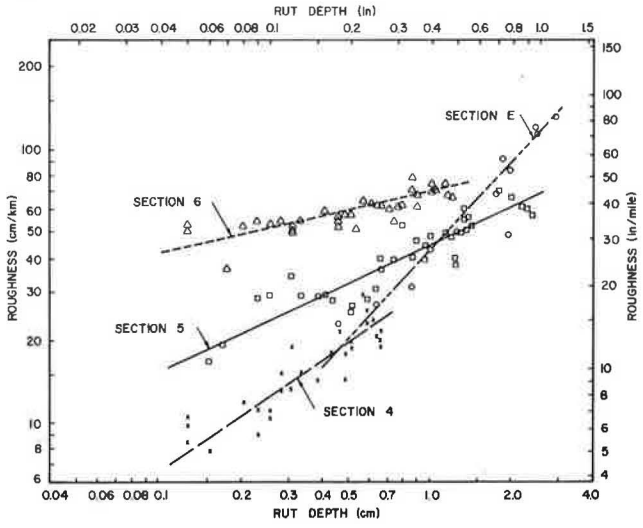

in 6 of 12 bituminous-concrete pavements, which included sections 1a, 1b, 1c, 1d, 8, and 9; however, no such type of cracking was observed in the pavements containing a crushed-stone, aggregate-lime-pozzolan, or aggregate-bituminous base. Among the many test pavements, potholes developed only in the aggregate-lime-pozzolan pavement. Details on the development of potholes have already been reported (17).

Class 2 and class 3 cracking developed in most test pavements. Previous papers (16,17) have described in detail the development and growth of surface cracking in the aggregate-cement, aggregate-lime-pozzolan, and crushed-stone pavements. Table 3 summarizes the number of EALs at 10 m^2/1000 m^2 of the entire pavement surface area, the number of EALs at crack initiation at the bottom of the base course, the number of EALs for crack propagation from the bottom of the base course to the top of the surface course, and the initial maximum tensile strain at the bottom of the base course for all cracked test pavements.

The rate of growth of the cracked area given in Table 3 was estimated by fitting the field data. Since the rate of growth in most cases is slow at the initial stage and increases at a greater rate, the values given are approximate average rates of crack propagation. The number of EALs at crack initiation was evaluated in the following way. First, the tensile strain at the bottom of the base course was computed by using the BISAR computer program together with the elastic moduli already determined for the spring conditions. The computed tensile strain varied with the number of EALs in a shape that resembles the variation of Benkelman-beam spring-season deflection. Second, the fatigue line of each base-course material was plotted. Finally, the approximate number of EALs for crack initiation at the bottom of the base course was obtained from the intersection of each fatigue line and the corresponding tensile-strain curve.

The difference between the number of EALs at crack initiation and that at a crack area of 10 m^2/1000 m^2 equals approximately the rate of crack propagation from the bottom of the base course to the top of the surface layer. The crack area of 10 m^2/1000 m^2 of entire pavement surface area was chosen arbitrarily. This amount of cracking corresponds to a PSI drop of about 0.6, as will be shown later. Relating the rate of crack propagation to the combined thickness of the base and surface layers yields the following approximate equation for rate of crack propagation:

$$(dC_l)/(dN) \cong 95.3 \exp(0.75\ N) \quad (5)$$

where C_l = the crack length (mm) and N = the number of EALs (000 000s). Note that Equation 5 was formulated by using the crack data obtained from the pavements that contained bituminous-concrete base only. Because the bituminous concrete in the base course is different from that in the surface layer and the surface-layer thickness varies at two different levels, 3.8 cm (1.5 in) and 6.4 cm (2.5 in), Equation 5 provides only a rough approximation of the average crack propagation through two different layers.

For the bituminous-concrete pavements, the rate of growth of the cracked area can be related to the maximum tensile strain at the bottom of the base course as follows:

$$(dC_a)/(dN) \cong 9.88 \times 10^{-12}\ \epsilon_t^{5.3} \quad (6)$$

where C_a = area of class 2 and class 3 cracking (m^2/1000 m^2) and ϵ_t = maximum tensile strain at the bottom of the base course (μm/m); thus,

Section 1d = 0.6×10^{-4},
Section 8 = 1.3×10^{-4},
Section 9 = 2.1×10^{-4},
Section H = 17.8×10^{-4},
Section 14 = 1.8×10^{-4},
Section A = 7.6×10^{-4},
Section C = 10.8×10^{-4},
Section D = 33.3×10^{-4},
Section 3 = 8.5×10^{-4},
Section 5 = 1.4×10^{-4}, and
Section E = 50.0×10^{-4}.

Therefore, it would be possible to estimate the degree of surface cracking at any time for the bituminous-concrete pavements by using Equations 5 and 6.

PAVEMENT PERFORMANCE

The PSI decreased with increasing number of EALs; the rate of decrease varied with such factors as base-course material, layer thickness, and EAL. In general, the shape of the performance curve followed the power function that was originally proposed by the American Association of State Highway Officials (18). As in the case of distress behavior, no significant variation in PSI between seasons was observed for the pavements studied. More detailed information on the change in PSI with EALs is given elsewhere (16,17,19).

Because the initial PSI values are generally low and vary considerably among pavements, this analysis considers only the difference in PSI that occurred after the initial measurements. Figure 7 presents the relationship between the maximum compressive strain on the top of the subgrade with the number of EALs for three levels of PSI drop, namely, ΔPSI = 0.5, 1.0, and 1.5. This figure indicates that a maximum value of compressive strain exists, so that the PSI drop after certain repetitions of EALs will not exceed any specified value. For the pavements that contain

Table 3. Crack data.

Section	Maximum Tensile Strain (μm/m)	Number of EALs at Crack Initiation (N_i) (000 000s)	Number of EALs at Crack Area of 10 m^2/1000 m^2 (N) (000 000s)	$N-N_i$ (000 000s)
1d	109.5	0.93	1.80	0.87
8	139.0	0.24	0.39	0.15
9	122.7	0.76	1.04	0.28
H	209.1	0.034	0.36	0.33
14	118.0	0.30	1.00	0.70
A	65.0	0.29	1.13	0.84
C	46.1	0.06	1.21	1.15
D	54.4	0.04	0.75	0.71
3	41.1	0.98	1.26	0.28
5	165.0	–	2.40	–
E	279.0	–	0.61	–

Note: 1 μm/m = 1×10^{-6} in/in; 1 m^2/1000 m^2 = 1 $yard^2$/1000 $yards^2$.

Figure 7. Initial maximum compressive strain versus EALs for various levels of PSI drop.

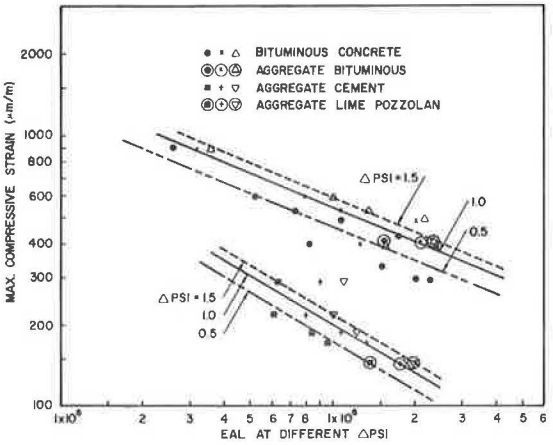

Figure 8. Rut depth versus PSI drop.

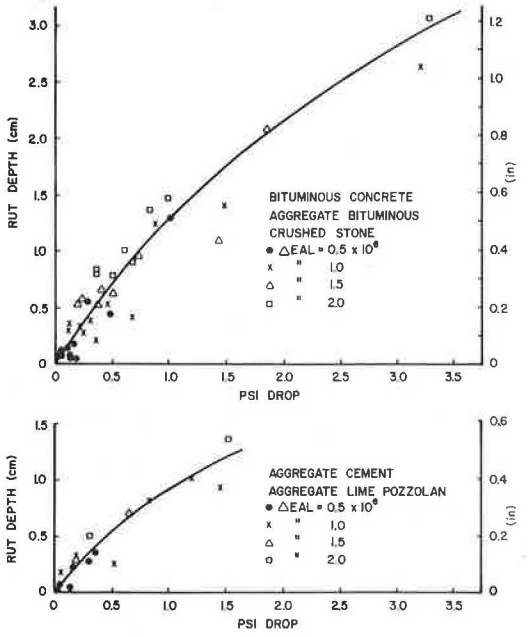

Figure 9. Surface roughness versus PSI drop.

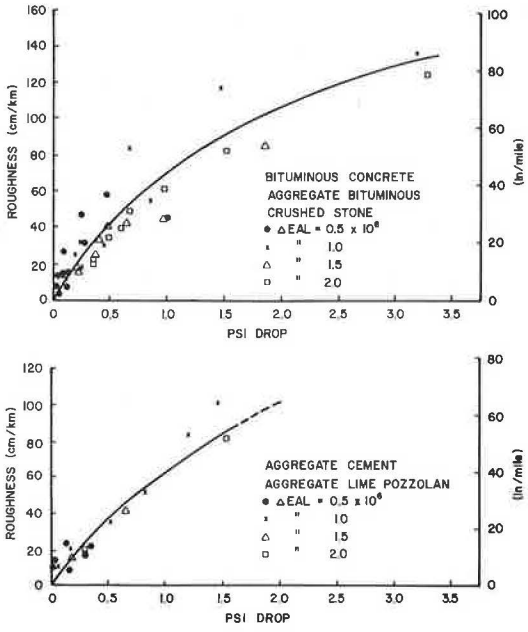

bituminous-concrete and aggregate-bituminous bases, the maximum compressive strains for ΔPSI = 0.5, 1.0, and 1.5 are approximately 460, 540, and 590 μm/m, respectively, at 1 million EALs. For aggregate-cement and aggregate-lime-pozzolan pavements, the maximum compressive strains are approximately 170, 200, and 240 μm/m for ΔPSI = 0.5, 1.0, and 1.5, respectively.

The PSI drops (ΔPSI) at 0.5, 1.0, 1.5, and 2.0 million EALs are related to the corresponding increases in rut depth (Figure 8), surface roughness (Figure 9), and area of surface cracking (Figure 10). Figures 8 and 9 demonstrate that the rate of increase with increasing ΔPSI for both rut depth and roughness becomes smaller at higher levels of ΔPSI. The reason for this is that, at higher ΔPSI values, cracking becomes more important in the determination of PSI, as depicted by Figure 10.

Figure 10. Area of surface cracking versus PSI drop.

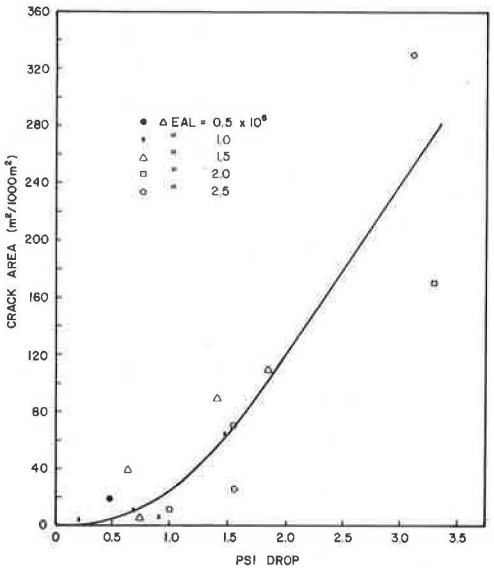

According to Figure 8, under the same levels of PSI drop, pavements whose bases contain bituminous concrete, aggregate bituminous, and crushed stone undergo greater rutting than do pavements whose bases contain aggregate cement and aggregate lime pozzolan. For the pavement bases that contain bituminous concrete, aggregate bituminous, and crushed stone, rut depths equal 0.71, 1.30, 1.78, and 2.16 cm (0.28, 0.51, 0.70, and 0.85 in), respectively, for ΔPSI = 0.5, 1.0, 1.5, and 2.0. Rut depths corresponding to the same levels of ΔPSI are 0.56, 0.91, 1.19, and 1.47 cm (0.22, 0.36, 0.47, and 0.58 in) for the pavement bases that contain aggregate cement and aggregate lime pozzolan. It is noteworthy that the rut depth at ΔPSI = 0.5 is very close to 6.4 mm (0.25 in) for all test pavements. This particular level of rutting has been widely used as an allowable rut depth in the design of high-quality highway pavements (20,21).

Figure 9 demonstrates that roughness changes for ΔPSI = 0.5, 1.0, and 1.5 are almost equal, regardless of the type of base-course material. The values of roughness are approximately 39.5, 71.0, and 94.7 cm/km (25, 45, and 60 in/mile) for ΔPSI = 0.5, 1.0, and 1.5, respectively. Based on Figure 10, the areas of surface cracking corresponding to ΔPSI = 0.5, 1.0, 1.5, and 2.0 are approximately 5, 25, 65, and 120 $m^2/1000\ m^2$ in terms of the entire pavement surface area, respectively. These levels of various distress manifestations and various levels of PSI drop might be used as a guide for selecting allowable distress levels for pavement design.

SUMMARY AND CONCLUSIONS

Rutting, roughness, and surface cracking of flexible pavements that contain five different base-course materials were discussed. The distress behavior was related to pavement response, which was analyzed by using the BISAR computer program. The distress behavior was also related to PSI values to establish the level of each mode of distress manifestation that corresponded to each level of PSI drop.

From this study, various equations that permit prediction of pavement distress from pavement response were developed. Also, allowable subgrade compressive strains to limit different distress modes within specific levels were established. The results of this study may be useful in selecting allowable distress levels and strain criteria for pavement design and also may be helpful in developing the relationship between distress and performance.

ACKNOWLEDGMENT

The study presented here is a part of a research project sponsored by the Pennsylvania Department of Transportation in cooperation with the Federal Highway Administration, U.S. Department of Transportation. Their support is gratefully acknowledged. The field data reported here were collected and reduced with the assistance of W. P. Kilareski, S. A. Kutz, B. A. Anani, R. P. Anderson, and P. J. Kersavage. This paper represents our views and does not necessarily reflect those of the Pennsylvania Department of Transportation or the Federal Highway Administration.

REFERENCES

1. F. N. Finn. Observation of Distress in Full-Scale Pavements. In Structural Design of Asphalt Concrete Pavement Systems, HRB, Special Rept. 126, 1971, pp. 86-90.
2. J. B. Rauhut, F. L. Roberts, and T. W. Kennedy. Response and Distress Models for Pavement Studies. TRB, Transportation Research Record 715, 1979, pp. 7-14.
3. J. B. Rauhut and P. R. Jordahl. Effects on Flexible Highways of Increased Legal Vehicle Weights Using VESYS IIM. Federal Highway Administration, U.S. Department of Transportation, Final Rept. FHWA-RD-77-134, Jan. 1978.
4. F. N. Finn, C. Saraf, R. Kulkarni, K. Nair, W. Smith, and A. Abdullah. Development of Pavement Structural Subsystems. NCHRP Project 1-10B, Final Rept., Feb. 1977.
5. A. I. M. Claessen, J. M. Edwards, P. Sommer, and P. Ugé. Asphalt Pavement Design—The Shell Method. Proc., 4th International Conference on Structural Design of Asphalt Pavements, Univ. of Michigan, Ann Arbor, Aug. 1977, pp. 39-74.
6. F. R. P. Meyer, A. Cheetham, and R. C. G. Haas. A Coordinated Method for Structural Distress Predictions in Asphalt Pavements. Presented at Annual Meeting, AAPT, Lake Buena Vista, FL, Feb. 1978.
7. E. S. Lindow, W. P. Kilareski, G. Q. Bass, and T. D. Larson. Construction, Instrumentation, and Operation. Pennsylvania Transportation Institute, Pennsylvania State Univ., University Park, Interim Rept. PTI 7504, Vol. 2, Feb. 1973.
8. W. P. Kilareski, S. A. Kutz, and G. Cumberledge. Modification, Construction, and Instrumentation of an Experimental Highway. Pennsylvania Transportation Institute, Pennsylvania State Univ., University Park, Interim Rept. PTI 7607, April 1976.
9. J. G. Hopkins. Pavement Roughness and Serviceability. Bureau of Materials, Testing, and Research, Pennsylvania Department of Transportation, Final Rept., Aug. 1975.
10. W. P. Kilareski, B. Anani, R. P. Anderson, M. C. Wang, and T. D. Larson. Remaining Life and Overlay Thickness Design for Modified Flexible Pavements. Pennsylvania Transportation Institute, Pennsylvania State Univ., University Park, Interim Rept. PTI 7905, Jan. 1979.
11. M. C. Wang, T. D. Larson, A. C. Bhajandas, and G. Cumberledge. Use of Road-Rater Deflections in Pavement Evaluation. TRB, Transportation Research Record 666, 1978, pp. 32-39.
12. K. Nair, W. S. Smith, and C. Y. Chang. Characterization of Asphalt Concrete and Cement-Treated Granular Base Course. Federal Highway Administration, U.S. Department of Transportation; Materials Research and Development, Inc., Oakland, CA, Final Rept., Feb. 1972.
13. S. Kolias and R. I. T. Williams. Cement-Bound Road Materials: Strength and Elastic Properties Measured in the Laboratory. Transport and Road Research Laboratory, Crowthorne, Berkshire, England, TRRL Supplementary Rept. 344, 1978.
14. Lime-Fly Ash-Stabilized Bases and Subbases. NCHRP, Synthesis of Highway Practice 37, 1976.
15. C. L. Saraf, W. S. Smith, and F. N. Finn. Rut Depth Perception. TRB, Transportation Research Record 616, 1976, pp. 9-14.
16. M. C. Wang and W. P. Kilareski. Behavior and Performance of Aggregate-Cement Pavements. TRB, Transportation Research Record 725, 1979, pp. 67-73.
17. M. C. Wang and W. P. Kilareski. Field Performance of Aggregate-Lime-Pozzolan Base Materials. TRB, Transportation Research Record 725, 1979, pp. 74-80.
18. The AASHO Road Test: Report 5—Pavement Research. HRB, Special Rept. 61E, 1962.
19. M. C. Wang and T. D. Larson. Evaluation of Structural Coefficients of Stabilized Base-Course Materials. TRB, Transportation Research Record 725, 1979, pp. 58-67.
20. C. L. Monismith and D. B. McLean. Structural Design Considerations. Proc., AAPT, Vol. 41, 1972, pp. 258-305.
21. G. M. Dormon and T. Metcalf. Design Curves for Flexible Pavements Based on Layered System Theory. HRB, Highway Research Record 71, 1965, pp. 69-84.

Publication of this paper sponsored by Committee on Flexible Pavement Design.

Nonlinear Characterization of Granular Materials for Asphalt Pavement Design

A. F. STOCK AND S. F. BROWN

In view of the well-established nonlinear resilient properties of unbound granular materials, analytically based pavement-design procedures should take proper account of this characteristic. The importance of including a failure criterion in the nonlinear model is demonstrated; the potentially high modulus of granular materials is not being realized in situ because of the unfavorable stress conditions that develop. The nonlinear model that has been written into the pavement-design computer program ADEM is described, and typical results are presented and compared with those based entirely on linear-elastic analysis. The results show that the thickness and quality of granular material have only a minor influence on the required thickness of asphalt but that, for accurate design, nonlinear analysis is required.

The development of a computer program for the design of asphalt pavements by using analytical techniques has been reported (1). This program, ADEM, assumed all layers to be